Quantum-field coherence in a Raman amplifier

K. C. Yeong and Joseph W. Haus
Physics Department, Rensselaer Polytechnic Institute, Troy, New York 12180-3590

A. V. Chizhov
Bogoliubov Laboratory of Theoretical Physics, Joint Institute for Nuclear Research, 141980 Dubna, Russia

(Received 25 October 1995)

We investigate the dynamics of a two-mode stimulated Raman scattering model including propagation and the quantum correlations that develop between the Stokes and anti-Stokes fields. For example, under certain conditions two-mode squeezed states can result. We report results for quadrature squeezing and sum squeezing. Quadrature squeezing only occurs when the anti-Stokes coupling constant is larger than the Stokes coupling constant. The amount of squeezing increases as the damping of the material polarization is increased.

PACS number(s): 42.50.Dv,32.80.Cy,42.65.Dr

I. INTRODUCTION

Stimulated Raman scattering has provided a wealth of information about quantum statistics and field coherence [1]. Being an amplifier system, quantum noise is magnified to macroscopic levels and statistical properties are directly related to the quantum initiation of the Stokes field. Several physical properties have been examined in the context of quantum initiation including the quantum statistics of solitary wave generation [2,3], pulse energy statistics [4–9], beam-pointing statistics [1,10,11], and spectral properties [12,13].

The Stokes field undergoes a large amplification, but the noise level remains quantum limited, corresponding to one photon per spatiotemporal mode. As a result, Raman amplifiers have been used for quantum limited image amplification with possible applications to the medical field [14,15].

Few studies have reported the quantum dynamics of stimulated Raman scattering (SRS) when both the Stokes and anti-Stokes fields are important. Penzkoffer, Laubereau, and Kaiser [16] derived a formal expression for the SRS equations for the Stokes and anti-Stokes fields. They have studied the coupling between the two fields in the steady-state regime. Ackerhalt and Milonni [17] derived the SRS equations by treating the interaction as a four-wave mixing and have concentrated their work primarily in the studies of Raman solitons. Both of these studies ignore the quantum aspects of the field. Scalora, Bowden, and Haus [18] have studied the coupling of the pump, Stokes, and anti-Stokes fields with the inclusion of diffraction and quantum initiation effects.

In a previous paper [19], we have studied the quantum correlations between the Stokes and anti-Stokes fields using a single-mode model of the fields. This corresponds to a cavity model coupling between the fields and the atomic media. Solutions were obtained in the linear regime; the coherence functions were calculated to examine several types of quantum-squeezing phenomena, namely, quadrature squeezing and two types of higher-order coherences called sum and difference squeezing [20]. For that model only sum squeezing existed.

In this paper, we have extended the study to include the effects of propagation. First, we have studied the quantum initiation of the Stokes and anti-Stokes fields in a little more detail in Sec. II. In Sec. III, the equations for quadrature and sum squeezing are given for the continuum field case. We present the results we have obtained for the quantum correlation between the Stokes and anti-Stokes fields in Sec. IV.

II. MODEL

We treat multiple fields in SRS by including the coupling between three fields: the pump laser and two fields generated from its interaction with the medium, the Stokes and the anti-Stokes fields. The SRS equations for the two-mode Raman amplifier in the slowly varying envelope approximation with phase matching of the anti-Stokes field are

$$\frac{\partial E_L^{(+)}}{\partial \xi} = \beta Q^{(-)} E_A^{(+)} - \kappa Q^{(+)} E_S^{(+)}, \tag{1a}$$

$$\frac{\partial E_S^{(+)}}{\partial \xi} = \kappa Q^{(-)} E_L^{(+)}, \tag{1b}$$

$$\frac{\partial E_A^{(+)}}{\partial \xi} = -\beta Q^{(+)} E_L^{(+)}, \tag{1c}$$

$$\frac{\partial Q^{(+)}}{\partial \tau} = -\Gamma Q^{(+)} + \kappa N E_S^{(-)} E_L^{(+)} + \beta N E_A^{(+)} E_L^{(+)} + F^{\dagger}. \tag{1d}$$

These equations are similar to the ones used by Scalora, Bowden, and Haus [18] but here we neglect diffraction effects. We adopt the normalization convention used by Englund and Bowden [2] for the various fields and parameters that occur in the equations. That is, the fields in Eqs. (1) are dimensionless and the length of the medium is normalized to unity.

The variable $\xi = z$ is the propagation distance inside the medium and $\tau = t - z/c$ is the retarded time where c for all practical purposes equals the speed of light in vacuum. $E_L^{(+)}$, $E_S^{(+)}$, and $E_A^{(+)}$ in Eqs. (1) correspond to the laser

1050-2947/96/53(5)/3606(8)/$10.00

field, the Stokes field, and the anti-Stokes field, respectively. $Q^{(+)}$ is the macroscopic polarization of the medium and Γ is the collisional damping rate.

The symbols κ and β denote the coupling constants for the Stokes and anti-Stokes fields, respectively. The ratio of these coefficients distinguishes two regimes of dynamical evolution with distinct quantum coherence properties. The function Q is the effective transition operator; the process is driven by the Langevin force operator F, which is taken to be a Gaussian, Markovian, stationary random process and is further discussed below.

The system of equations with Stokes and anti-Stokes fields develops distinct coherence properties during evolution depending on the magnitude of the coupling constants, i.e., whether or not the Stokes coupling constant κ is dominant over the anti-Stokes coupling constant β. The laser field is assumed to be undepleted; i.e., the first equation of the set in Eqs. (1) is not relevant and $E_L^{(+)}$ is constant. The remaining equations are linear and can be solved by Laplace transform techniques. In the undepleted-pump regime, the solutions for the case of $\kappa > \beta$ follow naturally from Eqs. (1). They are given by

$$\begin{aligned} E_S^{(+)}(\xi,\tau) = {} & E_S^{(+)}(0,\tau) + \kappa \int_0^{\xi} d\xi' \, \widetilde{Q}^{(-)}(\xi,\tau;\xi',0) \\ & + \kappa^2 \int_0^{\tau} d\tau' \, \widetilde{E}_S^{(+)}(\xi,\tau;0,\tau') + \beta\kappa \int_0^{\tau} d\tau' \, \widetilde{E}_A^{(-)} \\ & \times (\xi,\tau;0,\tau') + \kappa \int_0^{\tau} \int_0^{\xi} d\tau' \, d\xi' \, \widetilde{F}(\xi,\tau;\xi',\tau'), \end{aligned} \tag{2}$$

$$\begin{aligned} E_A^{(+)}(\xi,\tau) = {} & E_A^{(+)}(0,\tau) - \beta \int_0^{\xi} d\xi' \, \widetilde{Q}^{(+)}(\xi,\tau;\xi',0) \\ & - \beta\kappa \int_0^{\tau} d\tau' \, \widetilde{E}_S^{(-)}(\xi,\tau;0,\tau') - \beta^2 \int_0^{\tau} d\tau' \, \widetilde{E}_A^{(+)} \\ & \times (\xi,\tau;0,\tau') - \beta \int_0^{\tau} \int_0^{\xi} d\tau' \, d\xi' \, \widetilde{F}^{\dagger}(\xi,\tau;\xi',\tau'), \end{aligned} \tag{3}$$

where the general definitions are employed:

$$\widetilde{E}_{A,S}^{(+)}(\xi,\tau;0,\tau') = \frac{N^{1/2} I_{OL}^{1/2}}{(\kappa^2-\beta^2)^{1/2}} e^{-\Gamma(\tau-\tau')} \xi^{1/2} \, \frac{I_1[\{4N(\kappa^2-\beta^2) I_{OL}(\tau-\tau')\xi\}^{1/2}]}{(\tau-\tau')^{1/2}} E_{A,S}^{(+)}(0,\tau'), \tag{4a}$$

$$\widetilde{Q}^{(+)}(\xi,\tau;\xi',0) = I_{OL}^{1/2} e^{-\Gamma\tau} I_0[\{4N(\kappa^2-\beta^2) I_{OL} \tau(\xi-\xi')\}^{1/2}] Q^{(+)}(\xi',0), \tag{4b}$$

$$\widetilde{F}(\xi,\tau;\xi',\tau') = I_{OL}^{1/2} e^{-\Gamma(\tau-\tau')} I_0[\{4N(\kappa^2-\beta^2) I_{OL}(\tau-\tau')(\xi-\xi')\}^{1/2}] F(\xi',\tau'). \tag{4c}$$

The pump field intensity is $I_{0L} = E_{0L}^2$ and E_{0L} is assumed to be real. The above solutions take on a familiar form when $\beta = 0$; they reduce to the solutions for the Stokes field.

Let us first examine the above solutions when $\kappa = 0$, i.e., when the laser-Stokes coupling is absent. This will be helpful in the following when both fields are present. In this case, only the anti-Stokes field exists and we can show that the normal-ordered intensity vanishes whereas the antinormal-ordered intensity is equal to the vacuum fluctuations. This is intuitively evident because the initiation of the anti-Stokes field in the medium requires the pump field E_L to excite the initial population from an excited state to a virtual state. This can happen if the pump field is far from resonance. As the population of the atoms returns to the ground state, a blue-shifted anti-Stokes field is emitted. The initiating radiation is then amplified as it travels along the Raman medium leading to stimulated Raman scattering. The asymmetry that exists between the Stokes and anti-Stokes intensities is due to the assumption in Eq. (1) that the initial population remains in the ground state. Since $\kappa = 0$, the population of the atoms remains in the ground state most of the time and hence the anti–Stokes field remains negligible.

When both the fields are present, the relative size of the coupling constants plays an important role in determining the magnitudes of the Stokes and anti-Stokes fields. If $\kappa > \beta$, we have the usual exponential growth in both the Stokes and anti-Stokes fields. This is because the strong coupling between the laser field and Stokes field is more effective in exciting the initial population from the ground state to a virtual state before it settles to an excited state. The process is then reversed due to the nonzero β, with the population of atoms going from the excited state to another virtual state and back to the ground state. This reversed process is driven by the polarization of the Raman medium.

If $\beta > \kappa$, we find that the pump field is less effective in driving the initial population of the ground state to the excited state. This is because the coupling between the pump field and the Stokes field is smaller than that of the laser and anti-Stokes, and the anti-Stokes field removes population from the excited state and thus reduces the atomic polarization. Since the initial averages are defined such that the initial population is in the ground state, the buildup of the Stokes field will be small. This implies a small generation of the anti-Stokes field that results from the weakened induced polarization in the Raman medium. Therefore, the dynamics of the system when $\beta > \kappa$ shows that the magnitudes of the fields are smaller and the buildup is slower compared to the previous state.

The solutions for E_S and E_A when $\beta > \kappa$ have the same general form as Eqs. (2) and (3) but with $\kappa^2 - \beta^2$ replaced by

$\beta^2-\kappa^2$ and the modified Bessel function $I_n(x)$ replaced by the ordinary Bessel functions $J_n(x)$. This means that $\widetilde{E}^{(+)}_{A,S}(\xi,\tau;0,\tau')$, $\widetilde{Q}^{(+)}(\xi,\tau;\xi',0)$, and $\widetilde{F}(\xi,\tau;\xi',\tau')$ in Eq. (4) become

$$\widetilde{E}^{(+)}_{A,S}(\xi,\tau;0,\tau')=\frac{N^{1/2}I_{OL}^{1/2}}{(\beta^2-\kappa^2)^{1/2}}e^{-\Gamma(\tau-\tau')}\xi^{1/2}\,\frac{J_1[\{4N(\beta^2-\kappa^2)I_{OL}(\tau-\tau')\xi\}^{1/2}]}{(\tau-\tau')^{1/2}}E^{(+)}_{A,S}(0,\tau'), \tag{5a}$$

$$\widetilde{Q}^{(+)}(\xi,\tau;\xi',0)=I_{OL}^{1/2}e^{-\Gamma\tau}J_0[\{4N(\beta^2-\kappa^2)I_{OL}\tau(\xi-\xi')\}^{1/2}]Q^{(+)}(\xi',0), \tag{5b}$$

$$\widetilde{F}(\xi,\tau;\xi',\tau')=E_{OL}e^{-\Gamma(\tau-\tau')}J_0[\{4N(\beta^2-\kappa^2)I_{OL}(\tau-\tau')(\xi-\xi')\}^{1/2}]F(\xi',\tau'). \tag{5c}$$

We defined the averages of the Stokes and anti-Stokes fields in our calculations as

$$\langle E^{(+)}_{S,A}(0,\tau)E^{(-)}_{S,A}(0,\tau')\rangle=\delta(\tau-\tau'). \tag{6}$$

Since we assume that the ground state is initially populated, the averages for Q and F at the boundaries are

$$\langle Q^{(+)}(\xi,0)Q^{(-)}(\xi',0)\rangle=N\delta(\xi-\xi'), \tag{7}$$

$$\langle F^{\dagger}(\tau,\xi)F(\tau',\xi')\rangle=2\Gamma N\delta(\tau-\tau')\delta(\xi-\xi'). \tag{8}$$

These averages are consistent with the electric field commutation relations. We can verify that the solutions of the operator equations (3)–(5) are consistent with the field commutation relations

$$[E_i^{(+)}(0,\tau),E_i^{(-)}(0,\tau')]=[E_i^{(+)}(\xi,\tau),E_i^{(-)}(\xi,\tau')]$$
$$=\delta(\tau-\tau'), \tag{9}$$

where $i=A,S$. The independence of the commutation relation on ξ can be proved [21] by showing that

$$\frac{\partial}{\partial\xi}[E_i^{(+)}(\xi,\tau),E_i^{(-)}(\xi,\tau')]=0, \tag{10}$$

and by substituting the ξ derivatives for the SRS equations of the anti-Stokes field.

Expanding the commutation relation and taking an average, we obtain

$$\langle E_i^{(+)}(\xi,\tau)E_i^{(-)}(\xi,\tau')\rangle-\langle E_i^{(-)}(\xi,\tau')E_i^{(+)}(\xi,\tau)\rangle$$
$$=\delta(\tau-\tau'), \tag{11}$$

that is, the difference between the antinormal-ordered intensity and the normal-ordered intensity is equal to the delta function.

III. QUANTUM-FIELD CORRELATIONS

One difficulty encountered in our calculation for the higher-order correlation functions is the divergent term that arises from the vacuum fluctuations of the Stokes and anti-Stokes fields, when equal times are assumed. Normal first-order squeezing does not have this problem as the divergent term cancels. However, in sum squeezing, the divergent term is present as a product with other nondivergent terms, as shown below. In order to avoid this problem, we have assumed that the correlation functions are measured at two different times.

A. Quadrature squeezing

Let us define the operators as a linear combination of the Stokes and anti-Stokes field operators:

$$X_1=\frac{1}{\sqrt{8}}[E_S^{(-)}(\xi,\tau)+E_A^{(-)}(\xi,\tau)+E_S^{(+)}(\xi,\tau)+E_A^{(+)}(\xi,\tau)], \tag{12a}$$

$$X_2=\frac{i}{\sqrt{8}}[E_S^{(-)}(\xi,\tau)+E_A^{(-)}(\xi,\tau)-E_S^{(+)}(\xi,\tau)-E_A^{(+)}(\xi,\tau)]. \tag{12b}$$

The standard deviations, ΔX_i, are constructed from both operators; their products satisfy the Heisenberg inequality

$$\Delta X_1\Delta X_2\geqslant\tfrac{1}{2}|\langle C_X\rangle|, \tag{13}$$

where C_X is the commutator $[X_1,X_2]$ that can be represented as a linear combination of the commutators $[E_S^{(+)}(0,\tau),E_S^{(-)}(0,\tau)]$ and $[E_A^{(+)}(0,\tau),E_A^{(-)}(0,\tau)]$. The operators are in a quantum state, said to be normal squeezed in the X_1 direction if the variance of X_1 satisfies the condition

$$(\Delta X_1)^2<\tfrac{1}{2}|\langle C_X\rangle|. \tag{14}$$

To determine whether the dynamics produces a squeezed state, we define the shifted variance

$$\delta X_1^2=(\Delta X_1)^2-\tfrac{1}{2}|\langle C\rangle|, \tag{15}$$

which is negative when the state is squeezed along the X_1 direction.

B. Sum squeezing

Sum squeezing is a particular type of higher-order squeezing motivated by the ability of two fields to generate sum frequencies through a nonlinear interaction in a medium [19]. For sum squeezing, we adopt the definition of Hillery [20], introducing the following operators:

$$V_1=\tfrac{1}{2}[E_S^{(-)}(\xi,\tau_1)E_A^{(-)}(\xi,\tau_1)+E_S^{(+)}(\xi,\tau_2)E_A^{(+)}(\xi,\tau_2)], \tag{16a}$$

$$V_2=\frac{i}{2}[E_S^{(-)}(\xi,\tau_1)E_A^{(-)}(\xi,\tau_1)-E_S^{(+)}(\xi,\tau_2)E_A^{(+)}(\xi,\tau_2)], \tag{16b}$$

where $\tau_2>\tau_1$. There is sum squeezing in the V_1 direction if

$$(\Delta V_1)^2<\frac{C}{4}\langle E_S^{(-)}(\xi,\tau_1)E_S^{(+)}(\xi,\tau_2)+E_A^{(-)}(\xi,\tau_1)E_A^{(+)}(\xi,\tau_2)+C\rangle, \tag{17}$$

where

$$C=[E_S^{(+)}(\xi,\tau_1),E_S^{(-)}(\xi,\tau_2)]$$

or

$$[E_A^{(+)}(\xi,\tau_1),E_A^{(-)}(\xi,\tau_2)].$$

We similarly define the shifted variance for V_1 as

$$\delta V_1^2=(\Delta V_1)^2-\frac{C}{4}\langle E_S^{(-)}(\xi,\tau_1)E_S^{(+)}(\xi,\tau_2)+E_A^{(-)}(\xi,\tau_1)E_A^{(+)}(\xi,\tau_2)+C\rangle, \tag{18}$$

which is negative in the region of the quantum state. Since we have assumed $\tau_2>\tau_1$, then $C=\delta(\tau_1-\tau_2)=0$. Therefore, light is sum squeezed in the V_1 direction if

$$\delta V_1^2=(\Delta V_1)^2<0. \tag{19}$$

In the context of a single-mode SRS model, we have previously found the existence of sum squeezing in a case where quadrature squeezing was absent [19]. Thus, the absence of squeezing for the second moments cannot be used to preclude hidden quantum coherence properties that become apparent for higher moments.

There is another type of higher-order squeezing called difference squeezing [20] that is not reported here. As in our previous single-mode model [19], we did not find squeezing for those moments and therefore, they are not discussed further.

IV. RESULTS

We illustrate the calculations of the previous section for a variety of parameters. The parameters of interest in the model are the damping constant, the coupling constants, the retarded time, and the propagation distance along the Raman cell. The shifted variances, for the cases when the Stokes-laser coupling constant is larger than the anti-Stokes–laser coupling constant and vice versa, are examined against the model parameters for squeezing of light.

For all the results below, we have fixed the pump intensity at $I_{OL}=10^{22}$ and the number of Raman active molecules at $N=10^{22}$. The values of the coupling constants are $\kappa=2.0\times10^{-22}$, $\beta=10^{-22}$ when $\kappa>\beta$ and $\kappa=10^{-22}$, $\beta=2.0\times10^{-22}$ when $\beta>\kappa$. The parameters are taken from Ref. [2] although we have arbitrarily increased the pump intensity and the number of Raman active molecules to increase the magnitude of squeezing. The retarded time is

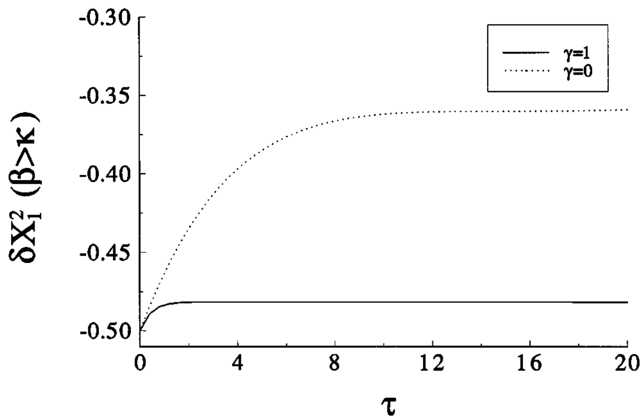

FIG. 1. The quadrature δX_1^2 defined in Eq. (15). For this case $\beta>\kappa$ and the propagation distance is $\xi=1.0$. The initial squeezing is largely decreased without damping $\Gamma=0$ and its value is retained for large damping $\gamma=1$. The symbol γ is defined in the Appendix.

scaled by $4N|\beta^2-\kappa^2|I_{OL}$ and γ is defined in the Appendix, Eq. (A4).

A. Quadrature squeezing

The solutions for the field operators in Eqs. (1) are applied in calculating the field moments to determine if the fields are quadrature squeezed in the sense of two-mode squeezing. We independently carried out the moment analysis for the Stokes field and anti-Stokes field and found that there is no first-order squeezing for the individual Stokes or anti-Stokes fields in either the uncoupled system or the coupled system. However, when a linear combination of the Stokes and anti-Stokes fields is used in the coupled system, then the light is squeezed for the first quadrature of the state $\beta>\kappa$.

Figure 1 is a plot of the shifted variances versus the retarded time for the first quadrature of the state $\beta>\kappa$. The figure is plotted at the propagation distance of $\xi=0.5$ for two values of γ. Light is X_i squeezed when the curve lies below the zero of the shifted variance δX_i^2. At time $\tau=0$ (local time), the shifted variance for this state is negative and the equation at this point is given by $\frac{1}{4}I_{0L}N\xi(-2\beta\kappa+2\kappa^2)$. The negative initial value for the variance is due to the quantum coherence that is built up between the field fluctuations at the boundary and the polarization fluctuations in the medium [see Eqs. (2) and (3)] as the fluctuations propagate into the medium. The curves for $\gamma=0$ and 1 show that light is X_1 squeezed for the length of time indicated. The amount of squeezing decreases in both instances. As γ increases from 0 to 1, the curve is asymptotically more negative; in other words as the material polarization damping increases, the amount of squeezing increases.

This happens because as we increase the damping constant, the polarization relaxes more quickly to follow the dynamics of the fields. In the limit of large damping, the polarization dynamics is adiabatically eliminated to give

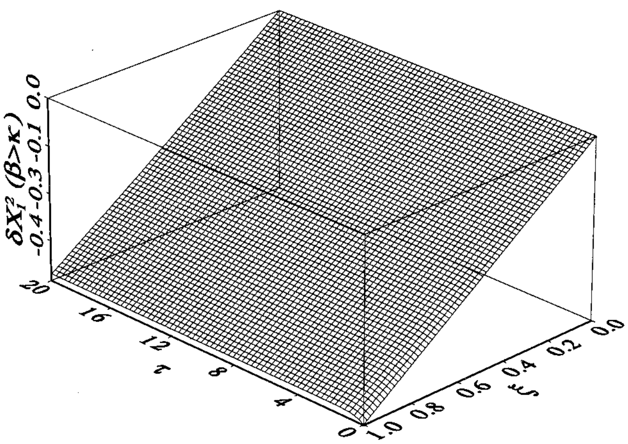

FIG. 2. A plot showing the variance δX_1^2 vs propagation distance and time. The damping constant is $\gamma=1$ and $\beta>\kappa$.

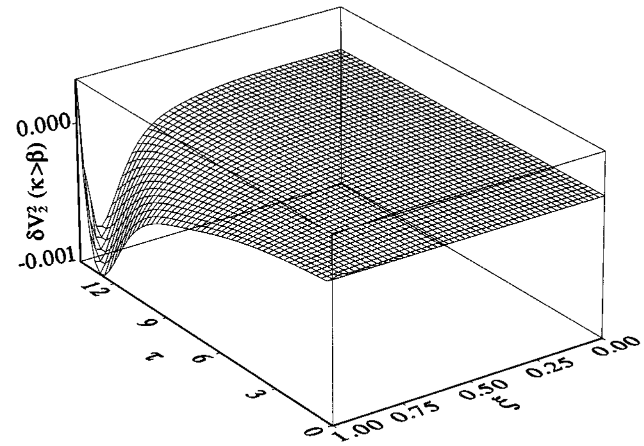

FIG. 3. The variance δV_2^2 for $\kappa>\beta$ and $\Gamma=0$. The initial vacuum state value is initially squeezed, but at longer times the squeezing is replaced by a positive shifted variance.

$$Q^{(+)}=\frac{\kappa}{\Gamma}NE_S^{(-)}E_L^{(+)}+\frac{\beta NE_A^{(+)}E_L^{(+)}}{\Gamma}+\frac{F^\dagger}{\Gamma}; \tag{20}$$

when this is substituted in Eqs. (1b) and (1c), the equations of motion resemble those for two-mode squeezing [22]:

$$\frac{dE_S^{(+)}}{d\xi}=\frac{NI_{0L}}{\Gamma}(\kappa^2E_S^{(+)}+\kappa\beta E_A^{(-)})+\frac{\kappa F}{\Gamma}, \tag{21}$$

$$\frac{dE_A^{(-)}}{d\xi}=-\frac{NI_{0L}}{\Gamma}(\kappa\beta E_S^{(+)}+\beta^2E_A^{(-)})-\frac{\beta F}{\Gamma}. \tag{22}$$

These are ordinary differential equations that describe the field quantum coherence in the adiabatic limit of large damping. The additional Langevin term limits the amount of squeezing. The dynamics of the fields for this case is oscillatory; as the laser places population to the excited state and the system amplifies the Stokes radiation, the stronger coupling of the anti-Stokes field generation returns it quickly to the ground state and reduces the amplification of the Stokes field. The two fields are in competition for the population.

The field strengths of the Stokes and anti-Stokes fields are limited due to the effect of the field competition on material polarization. The shifted variance is proportional to the correlation between the Stokes and anti-Stokes fields. Hence, as the damping constant increases, the intensity of the fields as well as of the two-field correlations decreases. Therefore, the shifted variance decreases.

Figure 2 is a three-dimensional plot of the shifted variance versus the propagation distance and the retarded time. We set $\gamma=1$, which is defined in the Appendix Eq. (A4); the integrals are numerically evaluated. It can be seen from the plot that squeezing increases as we increase the propagation distance and hold τ constant. It indicates that as the fields travel along the medium, the strength of the fields is more strongly correlated through their dynamics. This reduction in strength reduces the shifted variance.

B. Sum squeezing

Both cases of the coupling coefficients have the ability to develop sum-squeezed light. Some aspects of sum squeezing are found to be very similar to that of normal first-order squeezing. In the case of the system where $\kappa>\beta$, light was found to be squeezed in the variance of the operator V_2, whereas in the other case ($\beta>\kappa$) squeezing occurs in the variance of the operator V_1.

Despite the absence of quadrature squeezing for the case $\kappa>\beta$, there is sum squeezing. Figure 3 shows a three-dimensional plot of δV_2^2 versus the retarded time and the propagation distance for $\kappa>\beta$. We let $\tau_2=\tau_1+10^{-4}$ in our numerical representation of the analytical results. In this plot, $\Gamma=0$ and the light is squeezed over a range of times and distances. The $\tau=0$ values for the variance do not exhibit the field coherences discussed above for δX_1^2. However, the coherence that produces sum squeezing at later times is eventually destroyed and the squeezed variances show strong as-

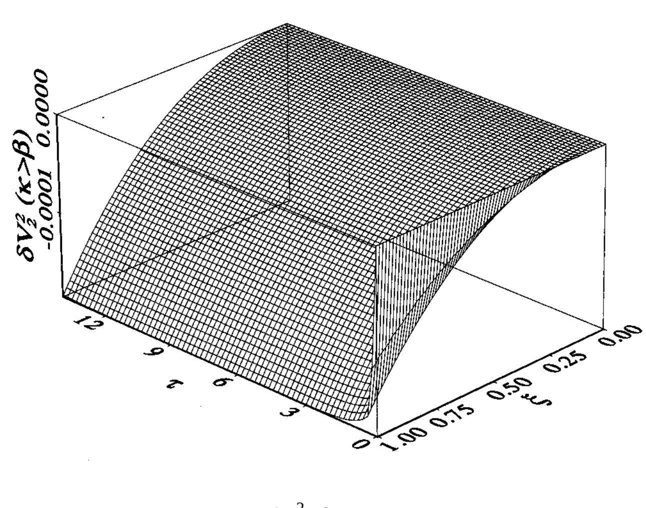

FIG. 4. The variance δV_2^2 for $\kappa>\beta$ and $\gamma=1$. The initial vacuum state value is squeezed and at longer times the shifted variance remains negative.

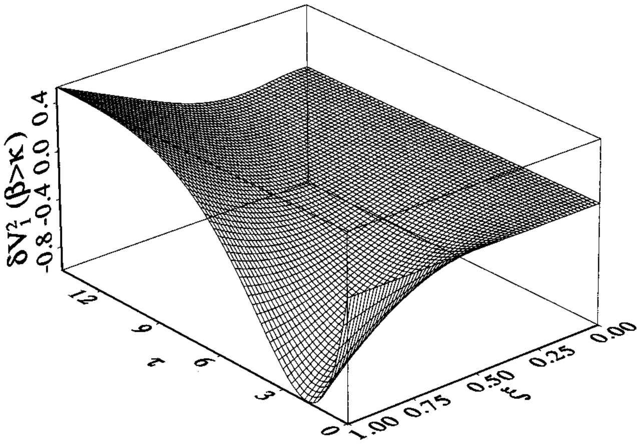

FIG. 5. The variance δV_1^2 for $\beta > \kappa$ and $\Gamma = 0$. The initial vacuum state value is initially squeezed, but at longer times the shifted variance is positive.

ymptotic growth towards infinity. This is due to the amplification of the noise in this case by the dynamics of the fields. The magnitude of the squeezing found is quite small; this is because the fields are not amplified for this case. The variance of V_1 is not squeezed for this case.

As Γ is increased, so too is the amount of squeezing, but only by a marginal amount. This is shown in Fig. 4, where δV_2^2 is plotted as a function of the propagation distance and time. In this plot, $\gamma = \Gamma / [4N(\kappa^2 - \beta^2) I_{0L}] = 1$ [defined in Eq. (A4)] and the integrals were numerically evaluated. The magnitude of the shifted variance has stabilized as a result of the increase of Γ. Light in this case is squeezed at longer times and larger distances. As for the case of quadrature squeezing above, the addition of damping serves to retain the coherence developed between the electromagnetic field operators. The additional dynamics of the polarization operator serves to eliminate the quantum coherence. Again, the operator V_1 does not exhibit squeezing.

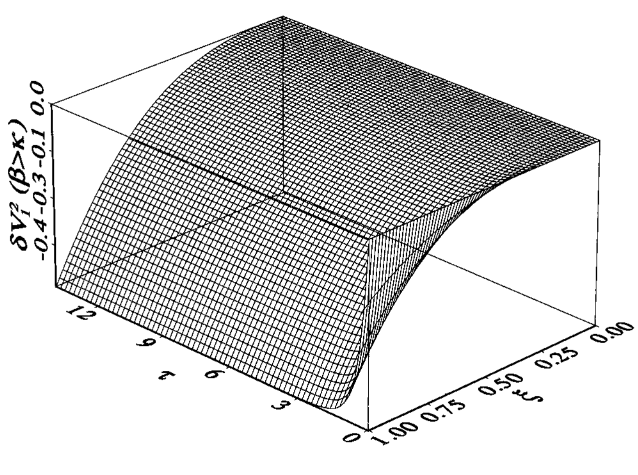

FIG. 6. The variance δV_1^2 for $\beta > \kappa$ and $\gamma = 1$. The initial vacuum state value is strongly squeezed and following by a saturation of the sum squeezing.

Despite the absence of quadrature squeezing for the case $\kappa > \beta$, there is sum squeezing. The three-dimensional space-time plot of δV_1^2 for this case with $\Gamma = 0$ is shown in Fig. 5. There is a substantial amount of squeezing at initial times as the light is propagating in the material. At long times though, the squeezing is eventually lost as the coherence is randomized. The much larger value for the minimum of the variance in this case, as compared with Fig. 3, is due to the amplification of the field amplitudes. For this case the operator V_2 is not squeezed.

The squeezing is again stabilized at long times as Γ is increased. This is shown in Fig. 6 where the squeezing with propagation distance is apparent. The magnitude of the squeezing is reduced somewhat over the minimum value found in Fig. 5. The value is due to the influence of the polarization Langevin forces that tend to smear the coherence.

V. SUMMARY

In an SRS system where the Stokes field is allowed to couple with the anti-Stokes field, quantum coherences develop between the fields and are manifested as quadrature squeezing, as well as higher-order squeezing. When $\kappa > \beta$, the light is sum squeezed. When $\Gamma = 0$, the magnitude of the shifted variance is large. As Γ is increased to unity, the magnitude of the shifted variance decreases significantly and the light is fully squeezed over a regime of space and time. When $\beta > \kappa$, the coherences develop normal first-order squeezing and sum squeezing. The magnitude of the shifted variance is smaller at $\Gamma = 0$ compared to the $\kappa > \beta$ case. When Γ is increased to unity, the magnitude of the shifted variance increases. This is in contrast to the case when $\kappa > \beta$ where the shifted variance decreases.

The sum squeezing is much larger in the case where $\beta > \kappa$, since the fields are not greatly amplified during propagation. The finding of sum squeezing for this case is reminiscent of our previous result for a nonpropagating field model [19], where sum squeezing was found without the appearance of quadrature squeezing.

APPENDIX

The following results have been used in the moment computations. They are provided here for the benefit of the interested reader. The calculations have used the following averages for the fields:

$$\langle E_{A,S}^{(+)}(0,\tau) E_{A,S}^{(-)}(0,\tau') \rangle = \delta(\tau - \tau'), \tag{A1a}$$

$$\langle Q^{(+)}(\xi,0) Q^{(-)}(\xi',0) \rangle = N \delta(\xi - \xi'), \tag{A1b}$$

$$\langle F^{\dagger}(\tau,\xi) F(\tau',\xi') \rangle = 2\Gamma N \delta(\tau - \tau') \delta(\xi - \xi'), \tag{A1c}$$

where N is the total number of Raman active molecules.

1. First-order normal squeezing

The two cases defined by the ratio of the coupling coefficients have identical derivations, so we report only one here. For the case $\kappa > \beta$, the shifted variance for the first quadrature is

$$\langle \delta X_1^2\rangle=\frac{1}{8}I_{OL}N\xi\Bigg\{-\beta\kappa[2e^{-2\gamma\tau}f_2(\tau,\xi)+4\gamma f_3(\tau,\xi)]+\kappa^2[e^{-2\gamma\tau}f_2(\tau,\xi)+1+2\gamma f_3(\tau,\xi)]-\beta^2[-1+e^{-2\gamma\tau}f_2(\tau,\xi)+2\gamma f_3(\tau,\xi)]-\frac{2\beta\kappa(\kappa^2+\beta^2-\beta\kappa)}{(\kappa^2-\beta^2)}f_1(\tau,\xi)+\frac{(\kappa^4+\beta^4)}{\kappa^2-\beta^4}f_1(\tau,\xi)\Bigg\}, \tag{A2}$$

where the following definitions are applied:

$$f_1(\tau,\xi)=\int_0^\tau d\tau' e^{-2\gamma(\tau-\tau')}\frac{I_1^2([\xi(\tau-\tau')]^{1/2})}{(\tau-\tau')}, \tag{A3a}$$

$$f_2(\tau,\xi)=I_0^2([\xi\tau]^{1/2})-I_1^2([\xi\tau]^{1/2}) \tag{A3b}$$

$$f_3(\tau,\xi)=\int_0^\tau d\tau' e^{-2\gamma(\tau-\tau')}I_0^2([\xi(\tau-\tau')]^{1/2})-I_1^2([\xi(\tau-\tau')]^{1/2}). \tag{A3c}$$

We have scaled the time coordinate τ and express it in units of $4N(\kappa^2-\beta^2)I_{OL}$, i.e., $\tau_{\rm new}=4N(\kappa^2-\beta^2)I_{OL}\tau_{\rm old}$ and the new damping constant is scaled according to

$$\gamma=\Gamma/4N(\kappa^2-\beta^2)I_{OL}. \tag{A4}$$

The pump field is assumed to be real and independent of τ. When $\beta>\kappa$, we replace $\kappa^2-\beta^2$ by $\beta^2-\kappa^2$ and the modified Bessel functions $I_n(x)$ by the ordinary Bessel functions $J_n(x)$.

2. Sum squeezing

For sum squeezing, the averages of the fields are made at two different times. The calculations for the shifted variances are similar to the first-order squeezing but with the addition of two-time correlations. For $\kappa>\beta$, the variance of the first quadrature has the following terms:

$$\begin{aligned}\langle[E_S^{(-)}(\xi,\tau_1)E_A^{(-)}(\xi,\tau_1)]^2\rangle&=\beta^2\kappa^2I_{OL}^2N^2\xi^2[e^{-4\gamma\tau_1}f_2^2(\tau_1)+4\gamma e^{-2\gamma\tau_1}f_2(\tau_1)f_3(\tau_1)-e^{-2\gamma\tau_1}f_2(\tau_1)-2\gamma f_3(\tau_1)+4\gamma^2f_3^2(\tau_1)]\\&+\frac{\kappa^2\beta^4}{(\kappa^2-\beta^2)}I_{OL}^2N^2\xi^2[2e^{-2\gamma\tau_1}f_2(\tau_1)f_1(\tau_1)-f_1(\tau_1)+4\gamma f_1(\tau_1)f_3(\tau_1)]\\&+\frac{\kappa^4\beta^2}{(\kappa^2-\beta^2)}I_{OL}^2N^2\xi^2[e^{-2\gamma\tau_1}f_2(\tau_1)f_1(\tau_1)-f_1(\tau_1)+2\gamma f_1(\tau_1)f_3(\tau_1)]\\&+\frac{\kappa^4\beta^4}{(\kappa^2-\beta^2)^2}I_{OL}^2N^2\xi^2f_1^2(\tau_1)+\frac{\kappa^2\beta^6}{(\kappa^2-\beta^2)^2}I_{OL}^2N^2\xi^2f_1^2(\tau_1)\end{aligned} \tag{A5a}$$

$$\begin{aligned}\langle[E_S^{(+)}(\xi,\tau_2)E_A^{(+)}(\xi,\tau_2)]^2\rangle&=\beta^2\kappa^2I_{OL}^2N^2\xi^2[e^{-2\gamma\tau_2}f_2^2(\tau_2)+2\gamma f_3(\tau_2)]\\&+\frac{\kappa^4\beta^2}{(\kappa^2-\beta^2)}I_{OL}^2N^2\xi^2[e^{-2\gamma\tau_2}f_2(\tau_2)f_1(\tau_2)+f_1(\tau_2)+2\gamma f_1(\tau_2)f_3(\tau_2)]\\&+\frac{\kappa^2\beta^4}{(\kappa^2-\beta^2)}I_{OL}^2N^2\xi^2f_1(\tau_2)+\frac{\kappa^4\beta^4}{(\kappa^2-\beta^2)^2}I_{OL}^2N^2\xi^2f_1^2(\tau_2)+\frac{\kappa^6\beta^2}{(\kappa^2-\beta^2)^2}I_{OL}^2N^2\xi^2f_1^2(\tau_2).\end{aligned} \tag{A5b}$$

To simplify the expression, the following notational definitions were introduced for the normal-ordered fourth moment $M_4^{\mathcal{N}}(\xi,\tau_1,\tau_2)=\langle E_S^{(-)}(\xi,\tau_1)\ E_A^{(-)}(\xi,\tau_1)\ E_S^{(+)}(\xi,\tau_2)\ E_A^{(+)}(\xi,\tau_2)\rangle$ and the antinormal-ordered fourth moment $M_4^{\mathcal{A}}(\xi,\tau_1,\tau_2)=\langle E_S^{(+)}(\xi,\tau_2)\ E_A^{(+)}(\xi,\tau_2)\ E_S^{(-)}(\xi,\tau_1)\ E_A^{(-)}(\xi,\tau_1)\rangle$ are given by the following lengthy expressions:

$$\begin{aligned}M_4^{\mathcal{N}}(\xi,\tau_1,\tau_2)&=\beta^2\kappa^2I_{OL}^2N^2\xi^2[e^{-2\gamma\tau_1}f_2(\tau_1)-1+2\gamma f_3(\tau_1)]\\&+\frac{\kappa^4\beta^2}{(\kappa^2-\beta^2)}I_{OL}^2N^2\xi^2[e^{-2\gamma\tau_1}f_2(\tau_1)f_1(\tau_2)-f_1(\tau_2)+2\gamma f_1(\tau_2)f_3(\tau_1)]\\&+\frac{\kappa^2\beta^4}{(\kappa^2-\beta^2)}I_{OL}^2N^2\xi^2f_1(\tau_1)+\frac{\kappa^4\beta^4}{(\kappa^2-\beta^2)^2}I_{OL}^2N^2\xi^2[f_4^2(\tau_1,\tau_2)+f_1(\tau_1)f_1(\tau_2)]\\&+\frac{2\kappa^4\beta^2}{(\kappa^2-\beta^2)}I_{OL}^2N^2\xi^{3/2}[e^{-\gamma(\tau_1+\tau_2)}f_5(\tau_1,\tau_2)+f_4^2(\tau_1,\tau_2)+2\gamma f_5(\tau_1,\tau_2)f_4(\tau_1,\tau_2)],\end{aligned} \tag{A6a}$$

$$M_4^{\mathscr{A}}(\xi,\tau_1,\tau_2)=\beta^2\kappa^2 I_{OL}^2 N^2\xi^2[e^{-2\gamma\tau_1}f_2(\tau_1)-1+2\gamma f_3(\tau_1)]+4\beta^2\kappa^2 I_{OL}^2N^2\xi[-e^{-2\gamma\tau_2}g(\tau_1,\tau_2)f_5(\tau_1,\tau_2)$$
$$-e^{-2\gamma(\tau_2-\tau_1)}g^2(\tau_1,\tau_2)+2\gamma g(\tau_1,\tau_2)f_5(\tau_1,\tau_2)e^{-\gamma(\tau_2-\tau_1)}]+\frac{\kappa^2\beta^4}{(\kappa^2-\beta^2)}I_{OL}^2N^2\xi^2 f_1(\tau_1)$$
$$+\frac{2\kappa^2\beta^4}{(\kappa^2-\beta^2)}I_{OL}^2N^2\xi^{3/2}g(\tau_1,\tau_2)e^{-\gamma(\tau_2-\tau_1)}f_4(\tau_1,\tau_2)+\frac{2\kappa^4\beta^2}{(\kappa^2-\beta^2)}I_{OL}^2N^2\xi^{3/2}[-e^{-\gamma(\tau_2-\tau_1)}g(\tau_1,\tau_2)f_4(\tau_1,\tau_2)$$
$$+e^{-\gamma(\tau_1+\tau_2)}f_4(\tau_1,\tau_2)f_5(\tau_1,\tau_2)+2\gamma f_4(\tau_1,\tau_2)f_5(\tau_1,\tau_2)]+\frac{\kappa^4\beta^2}{(\kappa^2-\beta^2)}I_{OL}^2N^2\xi^2$$
$$\times[e^{-2\gamma\tau_1}f_2(\tau_1)-f_1(\tau_1)+2\gamma f_1(\tau_2)f_3(\tau_1)]+\frac{\kappa^4\beta^4}{(\kappa^2-\beta^2)^2}I_{OL}^2N^2\xi^2[f_1(\tau_1)f_1(\tau_2)+f_4^2(\tau_1,\tau_2)]. \tag{A6b}$$

Additional moment contributions are

$$\langle E_S^{(-)}(\xi,\tau_1)E_A^{(-)}(\xi,\tau_1)\rangle=\kappa\beta I_{OL}N\xi[-e^{-2\gamma\tau_1}f_2(\tau_1)+1-2\gamma f_3(\tau_1)]-\frac{\kappa\beta^3}{(\kappa^2-\beta^2)}I_{OL}N\xi f_1(\tau_1) \tag{A7a}$$

$$\langle E_S^{(+)}(\xi,\tau_2)E_A^{(+)}(\xi,\tau_2)\rangle=-\kappa\beta I_{OL}N\xi-\frac{\kappa^3\beta}{(\kappa^2-\beta^2)}I_{OL}N\xi f_1(\tau_2), \tag{A7b}$$

where we introduced the following definitions

$$g(\tau_1,\tau_2)=\frac{I_1([\xi(\tau_2-\tau_1)]^{1/2})}{(\tau_2-\tau_1)^{1/2}}, \tag{A8a}$$

$$f_4(\tau_1,\tau_2)=\int_0^{\tau_1}d\tau'\,e^{-\gamma(\tau_1+\tau_2-2\tau')}\frac{I_1([\xi(\tau_1-\tau')]^{1/2})I_1([\xi(\tau_2-\tau')]^{1/2})}{(\tau_1-\tau')^{1/2}(\tau_2-\tau')^{1/2}}, \tag{A8b}$$

$$f_5(\tau_1,\tau_2)=\int_0^{\tau_1}d\tau'\,e^{-\gamma(\tau_1+\tau_2-2\tau')}i_0(\tau_1-\tau',\tau_2-\tau'), \tag{A8c}$$

$$i_0(\tau_1,\tau_2)=\frac{\tau_2{}^{1/2}I_0([\xi\tau_1]^{1/2})I_1([\xi\tau_2]^{1/2})-\tau_1{}^{1/2}I_1([\xi\tau_1]^{1/2})I_0([\xi\tau_2])}{\tau_2-\tau_1}. \tag{A8d}$$

The functions $g(\tau_1,\tau_2)$ and $f_4(\tau_1,\tau_2)$ result from the correlations between the Stokes and anti-Stokes fields. The functions $i_0(\tau_1,\tau_2)$ and $f_5(\tau_1,\tau_2)$ result from the correlations of the material polarization and the Langevin noise, respectively.

[1] M. G. Raymer and Walmsley, Prog. Opt. **28**, 183 (1990).
[2] J. C. Englund and C. M. Bowden, Phys. Rev. Lett. **57**, 2661 (1986); Phys. Rev. A **42**, 2870 (1990).
[3] D. C. MacPherson, R. C. Swanson, and J. L. Carlsten, Phys. Rev. A **40**, 6745 (1989).
[4] I. A. Walmsley, M. G. Raymer, T. Sizer II, I. N. Duling III, and J. D. Kafka, Opt. Commun. **53**, 137 (1985).
[5] K. Nattermann, N. Fabricius, and D. von der Linde, Opt. Commun. **57**, 212 (1986).
[6] A. S. Grabchikov, S. Ya. Kilin, V. P. Kazich, and N. M. Ido, Pis'ma Zh. Éksp. Fiz. **43**, 118 (1986) [JETP Lett. **43**, 151 (1986)].
[7] M. Lewenstein, Z. Phys. B **56**, 69 (1984).
[8] M. Scalora and J. W. Haus, Opt. Commun. **87**, 267 (1992).
[9] T. K. Tran and J. W. Haus, Phys. Rev. A **44**, 4608 (1991).
[10] M. Scalora, C. M. Bowden, and J. W. Haus, Phys. Rev. Lett. **69**, 3310 (1993).
[11] I. A. Walmsley, J. Opt. Soc. Am. B **8**, 8051 (1991); **8**, 2392(E) (1991).
[12] D. C. MacPherson, R. C. Swanson, and J. L. Carlsten, Phys. Rev. A **39**, 3487 (1989).
[13] J. C. Englund and C. M. Bowden, Phys. Rev. A **46**, 578 (1992).
[14] M. D. Duncan, R. Mahon, L. L. Tankersley, and J. Reintjes, Proc. SPIE **1626**, 325 (1992); **1409**, 127 (1991).
[15] J. A. Moon, M. D. Duncan, R. Mahon, and J. Reintjes, Opt. Lett. **19**, 1234 (1994).
[16] A. Penzkoffer, A. Laubereau, and W. Kaiser, Prog. Quant. Electron. **6**, 55 (1979).
[17] J. R. Ackerhalt and P. W. Milonni, Phys. Rev. A **33**, 3185 (1986).
[18] M. Scalora, C.M. Bowden, and J. W. Haus, Phys. Rev. A **48**, 3916 (1991).
[19] A. Chizhov, J. W. Haus, and K. C. Yeong, Phys. Rev. A **52**, 1698 (1995).
[20] M. Hillery, Phys. Rev. A **40**, 3147 (1989).
[21] L. You, J. Cooper, and M. Tippenbach, J. Opt. Soc. Am. B **8**, 1139 (1991).
[22] D. F. Walls and G. J. Milburn, *Quantum Optics* (Springer-Verlag, Berlin, 1994), p. 77.